Optical properties of polyvalent metals in the solid and liquid state: aluminium

1994 J. Phys.: Condens. Matter 6 2459

(http://iopscience.iop.org/0953-8984/6/13/008)

J. Phys.: Condens. Matter 6 (1994) 2459–2474. Printed in the UK

Optical properties of polyvalent metals in the solid and liquid state: aluminium

Bernd Hüttner

German Aerospace Research Establishment (DLR), Institut für Technische Physik, Pfaffenwaldring 38–40, 70569 Stuttgart, Germany

Received 10 September 1993, in final form 17 November 1993

Abstract. A semiphenomenological theory is proposed for the calculation of the frequency and temperature dependences of the optical properties of polyvalent metals. Utilizing the concept of parallel bands, the transverse optical conductivity is decomposed into a nearly-free-electron part and in an interband part. The theory needs only one fitting parameter, the unknown electron–electron scattering frequency above the Fermi energy. The complete set of optical quantities is calculated for aluminium for a large frequency range (0.01–50 eV) and from $T = 300$ to 2000 K.

1. Introduction

A complete knowledge of the 'optical constants' is desirable for many applications, e.g. for the treatment of materials by laser light. For this reason, many experiments have been made to determine the frequency dependence of the optical 'constants' refractive index and extinction coefficient or dielectric function of solid materials at a fixed temperature. Compilations are given by Palik (1985, 1989). However, only a few measurements exist for the temperature dependence of the absorption at a fixed wavelength (Miller 1969, Brückner *et al* 1989, Krishnan and Nordine 1993). The situation is still worse in the liquid state. Even for aluminium, presumably the most carefully investigated metal, our knowledge is far from being complete. As for the experiments, the reason lies in complications originating in surface contamination and in the high melting temperature of metals. As for the theory, it lies in the breakdown of translational invariance needed in the usual band-structure calculations. Although successful treatments to overcome this problem have been made recently by Hafner and co-workers (Hafner and Kahl 1984, Jank and Hafner 1990), the calculation of optical properties of liquid metals using the complete band structure is still left to the future. But even then, the computations would be rather time-consuming. For this reason, we propose a semiphenomenological theory for the frequency and temperature dependences of the optical properties of polyvalent metals in the liquid and solid state. In this paper, we restrict ourselves to the evaluation of aluminium. Other metals are treated in a forthcoming article.

The organization of this paper is as follows. In section 2, we outline the semiphenomenological theory for the calculation of transverse conductivity for cubic polyvalent metals. This is applied to solid and liquid aluminium in section 3. Conclusions and an outlook is contained in section 4.

0953-8984/94/132459+16$19.50

2. Theoretical model

The optical properties of metals are determined by the complex frequency- and temperature-dependent conductivity $\sigma(\omega, T)$. The relation with the complex dielectric function $\epsilon(\omega)$, commonly used for the calculation of the refractive index $n(\omega, T)$, extinction coefficient $k(\omega, T)$, reflection $R(\omega, T)$ and absorption $A(\omega, T)$, is given by

$$\epsilon(\omega, T) = 1 + \mathrm{i}4\pi\sigma(\omega, T)/\omega. \tag{1}$$

Following Ehrenreich (1966), we decompose the electronic conductivity into a nearly-free-electron (intraband) part $\sigma_{\mathrm{D}}(\omega, T)$ and an interband part $\sigma_{\mathrm{IB}}(\omega, T)$. Then we can write

$$\sigma(\omega, T) = \sigma_{\mathrm{D}}(\omega, T) + \sigma_{\mathrm{IB}}(\omega, T). \tag{2}$$

The second term can be rather involved for a complicated band structure because transitions for all energies are possible from flat bands lying below the Fermi energy level. Fortunately, the situation is somewhat simpler for polyvalent metals since near-parallel one-electron bands occur in these systems, contributing the dominant part to the interband conductivity. This is due to the much larger weight of the joint density of states to the transition probability for parallel bands. Here and in the following we neglect some additional fine structures arising at critical points. There have considerably smaller phase space and oscillator strengths (Ashcroft and Sturm 1971).

Taking this into account, we will approximate the interband contribution by a resonant-like term and the intraband conductivity by a Drude expression with a temperature-dependent relaxation time, $\tau_{\mathrm{D}}(T)$.

The well known Drude term for a time-dependent field reads

$$\sigma(\omega, T) = \sigma_{\mathrm{DC}}/[1 - \mathrm{i}\omega\tau_{\mathrm{D}}(T)] \tag{3}$$

where the DC conductivity σ_{DC} is given by

$$\sigma_{\mathrm{DC}}(T) = Ne^2\tau_{\mathrm{D}}(T)/m^* \tag{4}$$

with N as the density of conduction electrons and $m^* = Mm$ the effective electron mass. M is a measure for the deviation of the behaviour of the conduction electrons from that of true free electrons. The DC conductivity is related to the plasma frequency according to

$$\sigma_{\mathrm{DC}}(T) = \omega_{\mathrm{p}}^2\tau_{\mathrm{D}}(T)/4\pi M = \Omega_{\mathrm{p}}^2\tau_{\mathrm{D}}(T)/4\pi \tag{5}$$

where Ω_{p} is the plasma frequency of nearly free electrons.

The theoretical description of the interband conductivity in the present case is similar to the approach of Ehrenreich *et al* (1963), who derived straightforwardly an expression for $\sigma(\omega)$ from the assumption of a relaxation time from the Kubo formula. The problem of violation of the equation of continuity, which could appear by a naively constructed collision term, was first discussed by Ehrenreich (1966) and treated later in detail by Garik and Ashcroft (1980). In their paper the authors derived a number-conserving expression for the dielectric function, $\epsilon(\omega)$, which is somewhat more complicated than the formula used below in this paper. But numerical calculations for aluminium and sodium showed that the corrections are very small. This is especially valid for the range of available laser

frequencies being well below the plasma frequencies of metals and which, with respect to the applications, is of particular interest here.

In the relaxation-time approximation, the interband conductivity is given by (Ehrenreich 1966, Ashcroft and Sturm 1971)

$$\sigma_{IB}(\omega, T) = -i\frac{\omega_p^2(T)\omega}{4\pi}\sum_n \frac{A_n}{\omega_n^2 - [\omega + i/\tau_{IB}(T)]^2} \tag{6}$$

where

$$\omega_n = \omega_{lm} = \hbar^{-1}[E_l(k) - E_m(k)] \tag{7}$$

$$E_m(k) \leqslant E_F \leqslant E_l(k)$$

is the energy difference belonging to the nth parallel band, E_F is the Fermi energy level and ω is the photon energy. Further,

$$A_n = (2/m\hbar\omega_n)\langle p_{lm}^2\rangle \tag{8}$$

is an average oscillator strength and $\tau_{IB}(T)$ is the interband scattering time.

The index n counts the number of parallel bands and the energies $\hbar\omega_n$ are simply twice the Fourier component of the pseudopotential belonging to the respective interband transition. Since the calculation of these pseudopotential form factors is beyond the scope of a phenomenological theory, we will take over the values from existing band-structure calculations or from experiments, e.g. from the analysis of the de Haas-van Alphen effect (Ashcroft 1963).

Using the sum rule for the effective mass (Brust 1970, Smith and Shiles 1978), we derive in a non-local approximation a first equation for the determination of the oscillator strengths A_n, i.e.

$$\sum_n A_n = 1 - 1/M. \tag{9}$$

If we have only one parallel band, in the simplest approximation, equation (9) determines the oscillator strength if M is known. But in most cases two or three bands contribute and one needs further equations. These are given by

$$A_n/A_{n+1} = \mathrm{Re}\,\sigma_{IB}(\omega_n, T)/\mathrm{Re}\,\sigma_{IB}(\omega_{n+1}, T). \tag{10}$$

As can be easily shown by the determination of the maxima of the real part of the interband conductivity given by equation (6), equation (10) is valid for values for ω_n, not too closely spaced. In practice, these values may be taken from the measured interband conductivity or evaluated (see below) within the framework of the proposed theory.

In the limit $M \to 1$, equation (9) vanishes and thus indicates the fact that a free-electron gas cannot absorb photons. As a consequence, if in the liquid state the value of M is near unity, the interband contribution disappear, but for larger values they will be present. Thus equation (2) is applicable both in the solid state and in the liquid state.

Up to here, we have regarded the DC conductivity, the effective mass, the plasma frequency and the interband frequencies as constants and not as functions of the external parameters, temperature or pressure. This may be a usual and acceptable approximation

for small volume changes, but the experimental works of Tups and Syassen (1984) and Mathewson and Myers (1972) clearly show a remarkable pressure and temperature dependence, respectively, for all mentioned quantities. Since we are interested in the optical properties in the range from room temperature up to temperatures far above the melting point, where the temperature is mostly larger than the Debye temperature, we can describe the volume expansion by a linear approximation. Both in the solid and the liquid state we will take into account the volume dependence of the effective mass, the plasma frequency and the interband energies by its thermal expansion. A general expression reads

$$f(V) = f(V_0)(V_0/V)$$

where the volume V is given by

$$V(T) = V_0[1 + \beta_{s,l}(T - T_o)]$$

with the volume expansion coefficient $\beta_{s,l}$, where s refers to the solid state and l to the liquid one, respectively, and T_0 is an arbitrary reference temperature.

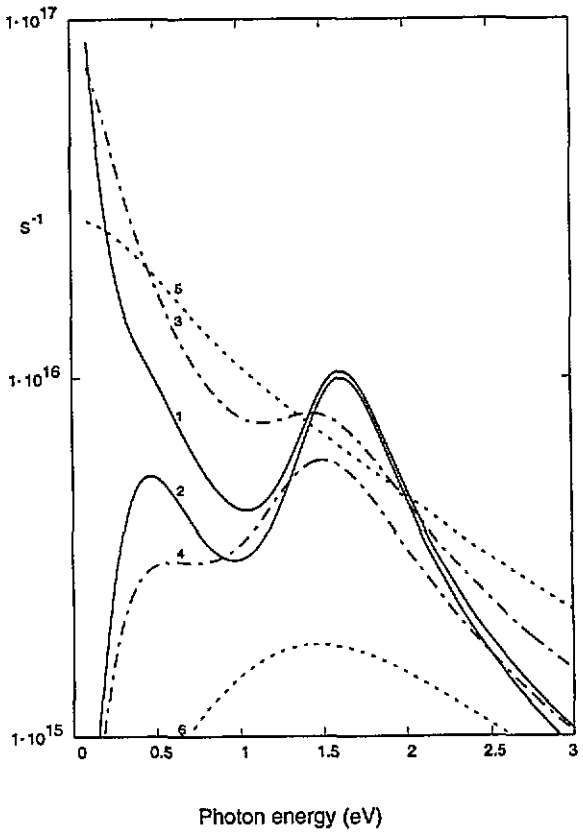

Figure 1. *Semilogarithmic plot of the real parts of the total conductivity and interband part of the* conductivity (in CGS units) at $T = 300$ K (1, 2:——), $T = 900$ K (3, 4:— · —) and $T = 1500$ K (5, 6:·····). The upper curve represents the total real conductivity at each temperature.

3. The optical properties of aluminium

For the temperature dependence of the DC electrical resistivity in the solid state, we can use in a good approximation

$$\rho_{\mathrm{DC,\,solid}}(T) = \rho_{\mathrm{DC,\,solid}}(T_0) + \beta_{\mathrm{DC,\,solid}}(T - T_0) \tag{11}$$

where a linear regression fit to the values of Ashcroft and Mermin (1976) gives for $\rho_{\mathrm{DC,\,solid}}$ and $\beta_{\mathrm{DC,\,solid}}$ the values 2.7437 $\mu\Omega$ cm and 0.0129 $\mu\Omega$ cm K^{-1}, respectively. A similar expression is valid for the liquid state,

$$\rho_{\mathrm{DC,\,liquid}}(T) = \rho_{\mathrm{DC,\,liquid}}(T_{\mathrm{m}}) = \beta_{\mathrm{DC,\,liquid}}(T - T_{\mathrm{m}}) \tag{12}$$

where from the work by Gathers (1983) we can take for the constants the value 24.23 $\mu\Omega$ cm and 0.0145 $\mu\Omega$ cm K^{-1}, respectively. The ratio of the liquid resistivity over the solid resistivity at the melting point represents a good check for the fitting relations used. Inserting the above values into equations (12) and (13) gives for the ratio 2.22, which exactly corresponds to the measured value (Iida and Guthrie 1988).

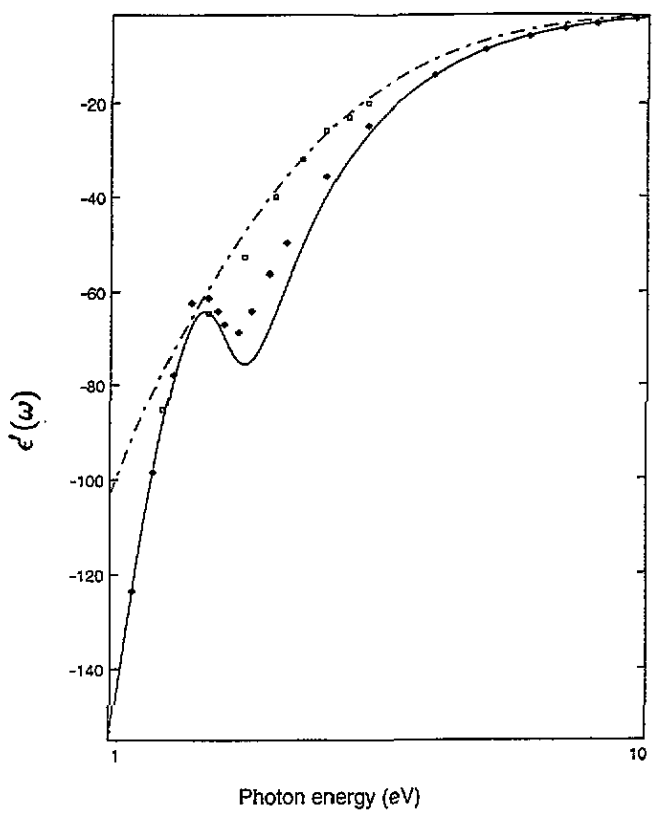

Figure 2. Real part of the dielectric function at $T = 300$ K (——) and $T = 1500$ K (— · —). Data points shown are taken from the work of Smith *et al* (1985) (♦) and Krishnan and Nordine (1993a) (□). Note that the x axis is logarithmic.

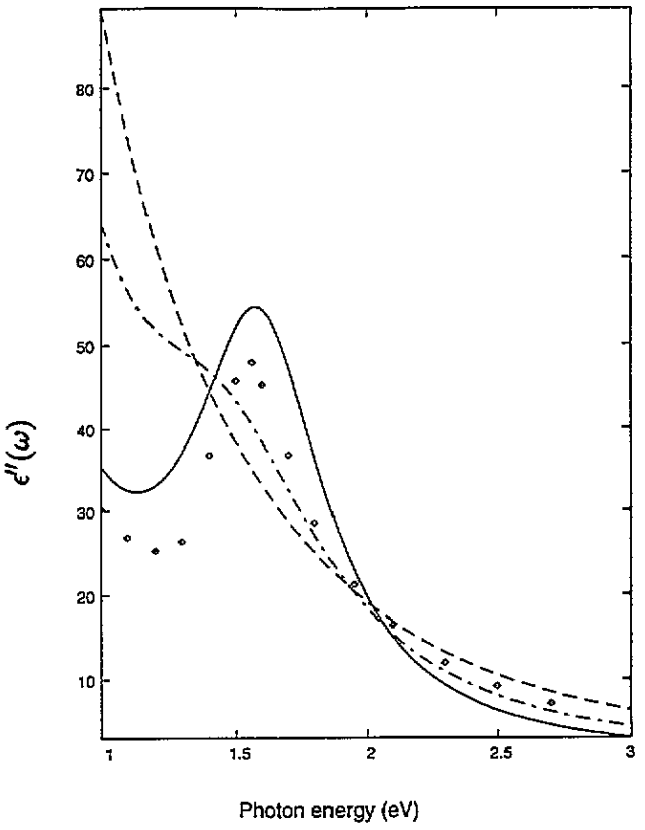

Figure 3. Imaginary part of the dielectric function at $T = 300$ K (——), $T = 900$ K (— · —) and $T = 1500$ K (– – –). Data points are from Smith *et al* (1985) (◊).

The volume dependence of the optical mass and of the band splittings was investigated by Tups and Syassen (1984). They found a nearly linear behaviour up to a very large change in volume (22%), which is much larger than the dilation between room temperature and the melting point caused by thermal expansion. This also justifies the linear regression fit, and we can write for the optical mass in the solid state

$$M_s(T) = M_s(T_0)/[1 + \beta_s(T - T_0)] \tag{13}$$

where the room-temperature value for the effective mass is taken from Mathewson and Myers (1972), $M_s(T = 300\ \text{K}) = 1.45$, and the thermal expansion is taken from e.g., Ashcroft and Mermin (1976), $\beta_s = 7.5 \times 10^{-5}\ \text{K}^{-1}$.

The behaviour in the liquid state is described by a similar expression

$$M_l(T) = M_l(T_m)/[1 + \beta_l(T - T_m)] \tag{14}$$

with the volume expansion coefficient $\beta_l = 1.5 \times 10^{-4}\ \text{K}^{-1}$ taken from Iida and Guthrie (1988). The value $M_l(T_m) = 1.28$ is calculated using equation (13) and taking into account the volume change (6.9%) at the melting point.

For the plasma frequency $\omega_p(T)$ we can use the same expressions if we substitute the denominator by its square root and insert 15.3 eV (Powell 1968) for the room-temperature value.

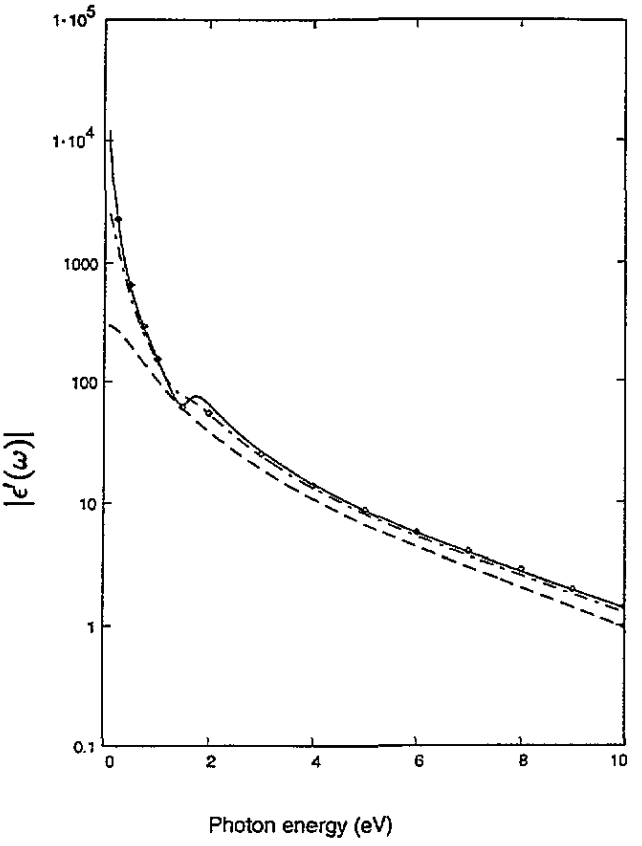

Figure 4. Magnitude of the real part of the dielectric function at $T = 300$ K (——), $T = 900$ K (— · —) and $T = 1500$ K (– – –). Data points are from Smith *et al* (1985) (◊). Note that the y axis is logarithmic.

Making use of equation (5), we are now able to calculate the Drude relaxation time in the solid and in the liquid state. Corrections to the scattering rate $1/\tau$, which may be due to surface scattering (Holstein 1952) or quantum effects, as pointed out by Gurzhi (1957), are not included since their contributions are negligible at higher temperatures.

It is easy to show that the magnitude of the real part of the interband conductivity in our model is proportional to the interband scattering time τ_{IB}. But a direct calculation of τ_{IB} is very complicated, even within the framework of more sophisticated theories, since it includes, among other effects, an ω-dependent electron–electron scattering and band-structure broadening (Sturm and Ashcroft 1974, Smith and Segall 1986). For this reason, we decompose τ_{IB}^{-1} into a temperature-dependent part described by the Drude relaxation time $\tau_D(T)^{-1}$, and a constant part τ_{ee}^{-1}, which is used as a fitting parameter. In other words, far above the Fermi energy an interband electron can be scattered by an electron–phonon interaction and additionally by an effective electron–electron interaction. This point should be stressed since a large phase space is available for the electron–electron scattering only for energies high above the Fermi level (Ashcroft and Mermin 1976). As a consequence, we used τ_{IB}^{-1} as a fitting parameter and got the best agreement with experiments for $\tau_{ee}^{-1}(300\text{ K}) = 4/\tau_D(300\text{ K})$. The necessity of different relaxation times was also pointed out by Benbow and Lynch (1975). It was impossible for the authors to obtain a reasonable

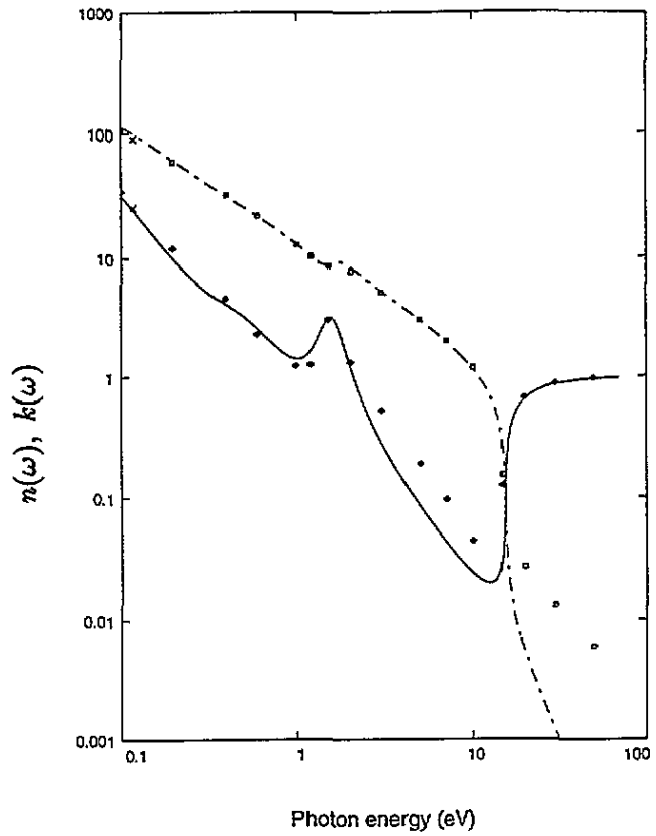

Figure 5. Refractive index (——) and extinction coefficient (— · —) at $T = 300$ K in a double-logarithmic plot. Data points are from Smith *et al* (1985): (♦) refractive index; (□) extinction coefficient.

fit to their conductivity data with only a single relaxation time.

The real part of the interband conductivity of aluminium shows two peaks around 0.3–0.4 eV and 1.6 eV (Smith *et al* 1985), and for the room-temperature values we will use $\omega_1 = 2U(111)/\hbar = 0.34$ eV and $\omega_2 = 2U(200)\hbar = 1.58$ eV (Tups and Syassen 1984). The temperature dependence of these energies is derived in the same manner as discussed above for the optical mass. The contributions to the peaks are due to the transitions between the second s-like and the third p-like bands along the directions U–Δ and K–Γ in k-space, respectively.

Inspecting the experimental curves (for example, see figure 6 of Ashcroft and Sturm (1971)) suggests for B, the ratio of the amplitudes of $\mathrm{Re}\,\sigma_{\mathrm{IB}}$ (equation (10)), the value $B \simeq 0.5$. Using the above values for ω_1, ω_2 and τ_{IB}, a numerical calculation yields $B = 0.56$.

Finally, the oscillator strengths are given by

$$A_1 = (1 - 1/M)[1/(1 + B)] \qquad A_2 = (1 - 1/M)[B/(1 + B)].$$

Now we have completed the list of quantities necessary for the computation of the optical functions.

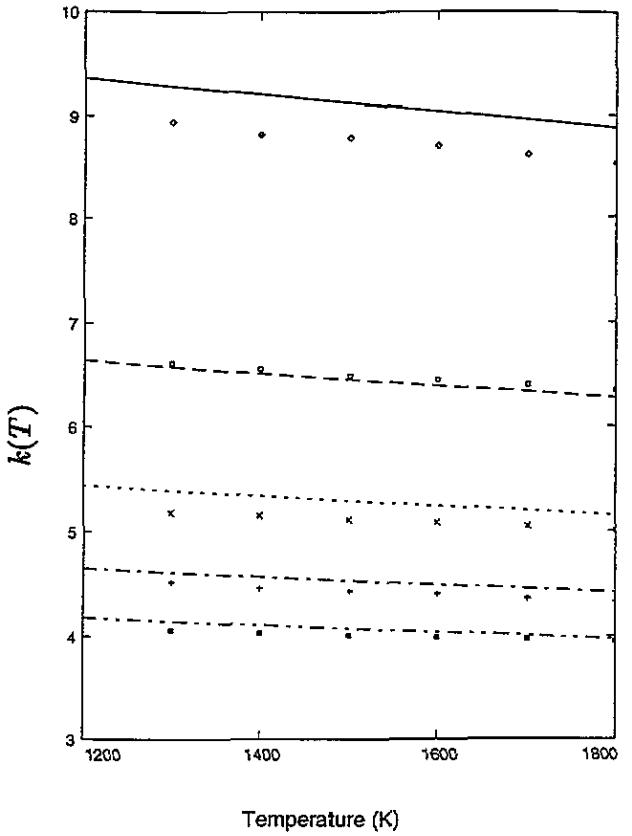

Figure 6. Extinction coefficient at $T = 1500$ K at five wavelengths: (— · · —) 381 nm, (— · —) 422 nm, (· · · · · ·) 500 nm, (– – –) 622 nm and (——) 968 nm. The data points are taken from Krishnan and Nordine (1993b): (■) 381 nm, (+) 422 nm, (×) 500 nm, (□) 625 nm and (◇) 968 nm.

By way of illustration, we plot in figure 1 the behaviour of the complete real part of the conductivity $\mathrm{Re}\,\sigma(\omega, T)$ and the interband contribution $\mathrm{Re}\,\sigma_{\mathrm{IB}}(\omega, T)$ at $T = 300, 900$, and 1500 K. As can be seen, the general effects of the temperature increase are to move the absorption peaks to lower energies and to broaden the peaks and reduce their heights due to the decreasing scattering time. The electron mean free path at $T = 1500$ K, calculated from the electron scattering time and the Fermi velocity, is around 20 Å for the intraband electrons and 14 Å for the interband electrons, respectively. This is in good agreement with the experimental results (Knight *et al* 1959) and supports our simple approximation for the scattering time.

The real and imaginary parts of the dielectric function, calculated from equation (1), are given in figures 2 and 3 and are compared with the available experimental results (Smith *et al* 1985, table XII, Krishnan and Nordine 1993b). Figure 4 shows the excellent agreement of the calculated $\mathrm{Re}\,\epsilon(\omega)$ with the experiment over a large range of photon energy. Note that the vertical scale is logarithmic.

The refractive index, $n(\omega) = \sqrt{[\mathrm{Re}\,\epsilon(\omega)]}$, and the extinction coefficient, $k(\omega) = \sqrt{[\mathrm{Im}\,\epsilon(\omega)]}$, are presented for $\omega = 0.01$–50 eV in figure 5. The small deviations at high energies could result from additional transitions, obtained in a self-consistent band-structure

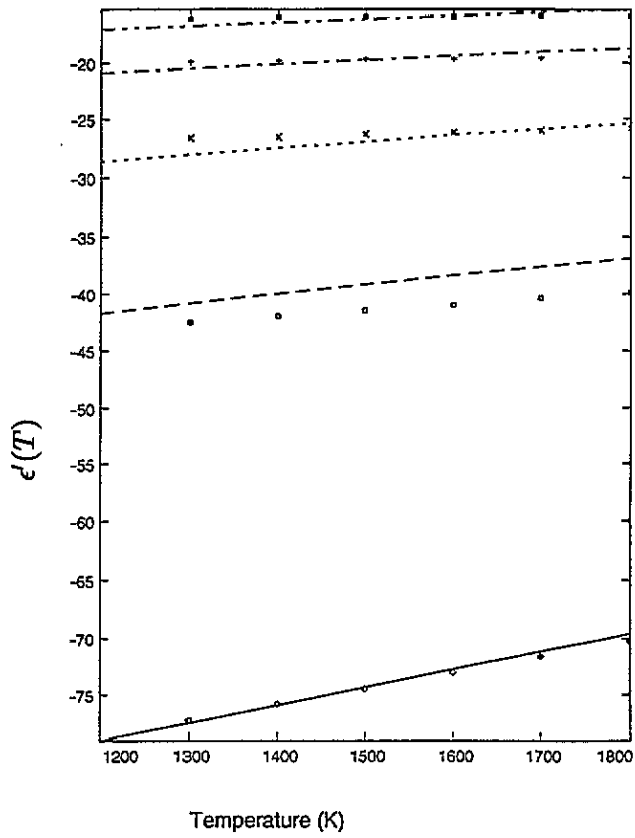

Figure 7. Real part of the dielectric function at $T = 1500$ K at five wavelengths: (— · · —) 381 nm, (— · —) 422 nm, (· · · · ·) 500 nm, (– – –) 622 nm and (——) 968 nm. The data points are taken from Krishnan and Nordine (1993b): (■) 381 nm, (+) 422 nm, (×) 500 nm, (□) 625 nm and (◇) 968 nm.

calculation by Alouani and Khan (1986), and/or by a redistribution of core oscillator strength resulting from exchange effects (Smith and Segall 1986). In figures 6 and 7 the extinction coefficient $k(T)$ and the real part of the dielectric function $\mathrm{Re}\,\epsilon(T)$ are plotted for five wavelengths together with the results from Krishnan and Nordine (1993b). Such a good agreement is not obtained for the refractive index, where the theory gives the correct qualitative temperature dependence but values higher by a factor of 1.5 to 2. Consequently, the same deviation appears for the real part of the conductivity because it is calculated by the authors from $n(T)$ and $k(T)$.

Before we enter into a detailed discussion of the frequency and temperature dependences of the optical absorption, first of all we should investigate the effective number of electrons per atom (e/at) contributing to the optical conductivity and the plasma frequency.

Among the different possibilities to define the effective number density by the partial f sums up to an energy ω, discussed by Smith and Shiles (1978), the most appropriate expression for our purpose reads

$$n_{\mathrm{eff}}(\omega, T) = \frac{2m}{\pi e^2 N_{\mathrm{a}}(T)} \int_0^{\omega} \mathrm{Re}\,\sigma(\omega', T)\,\mathrm{d}\omega' \tag{15}$$

since it is directly related to the energy dissipation of an electromagnetic wave. N_a represents the number of atoms per unit volume. Values of $n_{\text{eff}}(\omega, T)$ for the intraband and the complete oscillator strength are plotted in figure 8 for $\omega = 0$–10 eV at $T = 300, 900$ and 1500 K. As can be seen, our theoretical room-temperature values fit very well the experimental results $n_{\text{eff,intraband}} = 1.87 \pm 0.09$ and $n_{\text{eff,total}} = 2.78 \pm 0.09$, which are determined for the energy range 0–7 eV (Smith and Segall 1986). If we expand the energy integration up to 70 eV, just below the L edge at 72.65 eV, we get $n_{\text{eff,total}} = 2.84$, a value somewhat smaller than the expected valence conduction number of 3 e/at. This is not surprising, since we have taken into account only the contribution of parallel bands. The so-called normal interband transitions, which according to Ashcroft and Sturm (1971) yield an additional amount of the order of 10%, are neglected. But it is worth while to note that a simple comparison of the theoretical number with the experimental value, $n_{\text{total,exp.}} \sim 3.1$ e/at, must fail because core electrons are already involved in this high energy range.

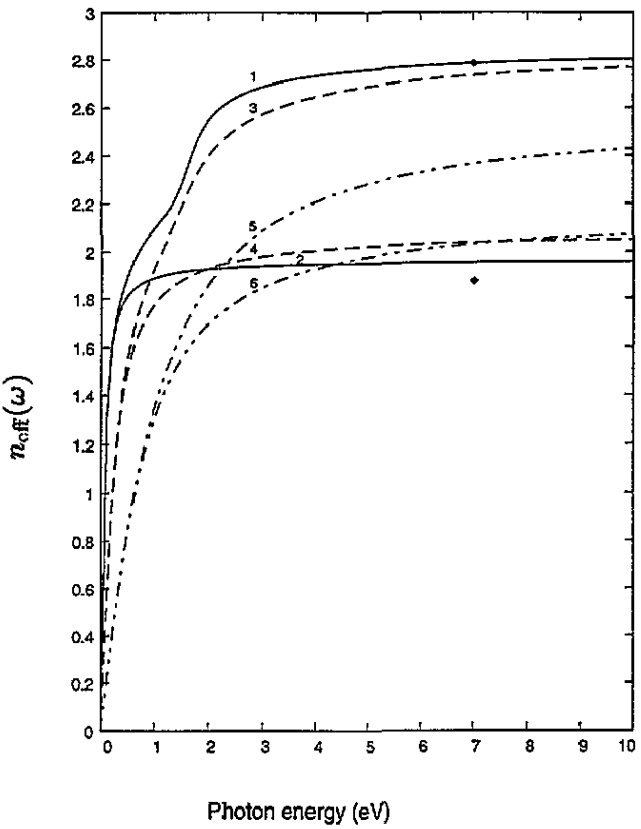

Figure 8. Effective density of electrons (in electrons per atom) for the total and the intraband conductivity at $T = 300$ K (1, 2: ——), $T = 900$ K (3,4: – – –) and $T = 1500$ K (5, 6: — · —). The experimental values at $T = 300$ K are taken from Smith *et al* (1985) (♦). At each temperature, the upper curve belongs to the total conductivity.

The comparison of the curves shows that with increasing temperature there is only a slight growth of the intraband absorption, in contrast to the much stronger decrease of the

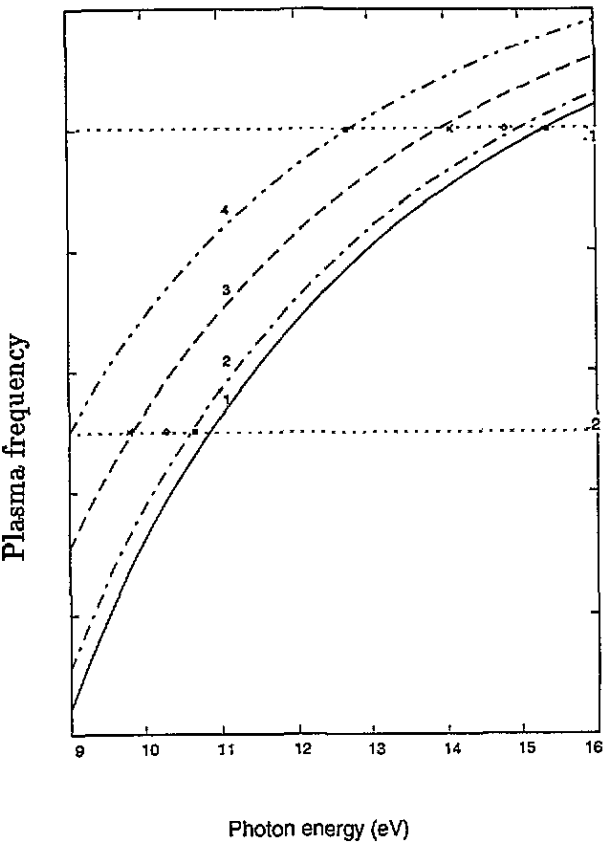

Figure 9. Volume and surface plasma frequency at $T = 300$ K (1: ——), $T = 900$ K (2: — · —) and $T = 1500$ K (3: - - - -). The intersection with -1 determines the volume plasma frequency and with -2 the surface plasma frequency. The plasma frequency of the nearly free electrons is given by curve 4 (— · · —). The data are taken from Powell (1968): (■) 300 K, (◇) 900 K and (×) 1500 K.

interband contribution. Evaluating the integral again up to 70 eV for $T = 1500$ K, we find an increase of the intraband contribution in comparison with the room-temperature value by a factor of 1.1 but a decrease of the interband term to $n_{\text{eff,interband}} = 0.40$. But more important than the reduction is the non-vanishing of this contribution. As a consequence, aluminium should possess a non-parabolic band structure also in the liquid state. Such a behaviour is well established for other metals, for example for lead from conductivity measurements by Inagaki *et al* (1982) and from band-structure calculations by Jank and Hafner (1990). Oelhafen *et al* (1988) have found structures in the density of states by means of ultraviolet photoelectron spectroscopy (UPS) measurements below the Fermi energy in some low-melting liquid metals.

The longitudinal plasma mode, which is measured, for example, in electron energy-loss experiments, has a frequency satisfying $\operatorname{Re}\epsilon(\omega) = 0$. The real part of the dielectric function is related to the imaginary part of the conductivity or to the polarizability, $\alpha(\omega)$, by

$$\operatorname{Re}\epsilon(\omega) = 1 + 4\pi \operatorname{Im}\sigma(\omega)/\omega = 1 + 4\pi\alpha(\omega). \tag{16}$$

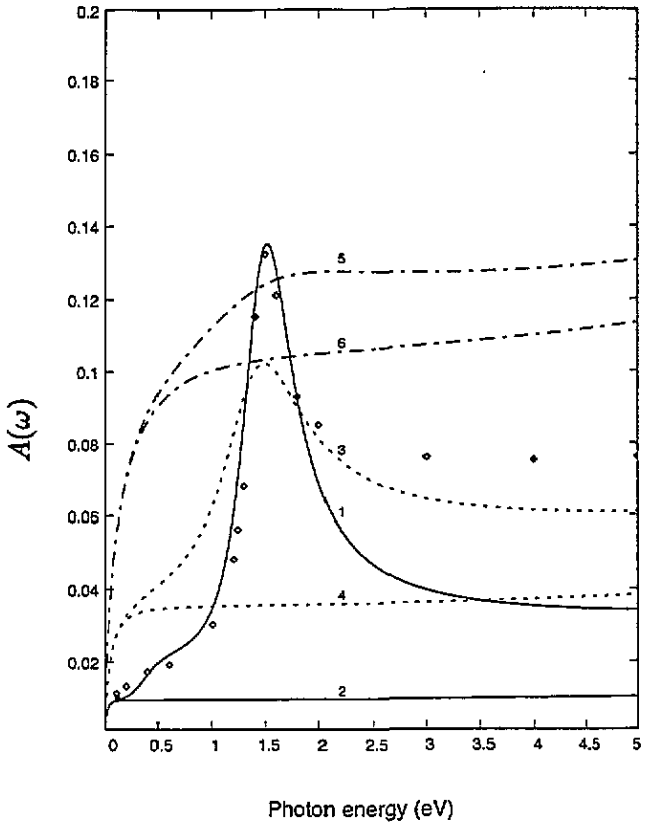

Figure 10. Total and Drude absorption at $T = 300$ K (1, 2: ——), 900 K (3, 4:· · · · · ·) and 1500 K (5, 6:— · —). The experimental values at $T = 300$ K are taken from Smith *et al* (1985) (◇) and from Brückner *et al* (1989) (■). The upper curves represent the total absorption.

Hence, the plasma frequency is determined in figure 9 as the frequency where the polarizability has the value -1. This is the case for the total polarizability at $\omega = 15.3$ eV and for the Drude part at $\Omega = 12.75$ eV. Additionally, the surface plasmons, excitable in thin metallic films, and determined by the intersection of $\alpha(\omega) = -2$, have the value $\omega_{ps} = 10.85$ eV. All values agree very well with the experimental results (Klemperer and Shepherd 1963, Smith *et al* 1985 table XI, Powell 1968).

We shall now consider absorption. In the case of transmissionless samples, an assumption valid for not too thin films, the absorption is given by

$$A(\omega, T) = 1 - R(\omega, T) = 1 - |[\epsilon(\omega, T) - 1]^{1/2}/[\epsilon(\omega, T) + 1]^{1/2}|. \qquad (17)$$

The electronic absorption (total and the Drude term) is plotted in figure 10 at $T = 300, 900$ and 1500 K. In contrast to the simple Drude behaviour, which is nearly constant from far-infrared (FIR) to ultraviolet (UV), the complete expression shows marked peak structure and a large enhancement around 1.5 eV in the solid state. For low energies, $\omega < 0.1$ eV, the graphs confirm the observation by Bennett *et al* (1963) that the free-electron Drude model gives a good account of the reflectance of aluminium. The change in absorption with

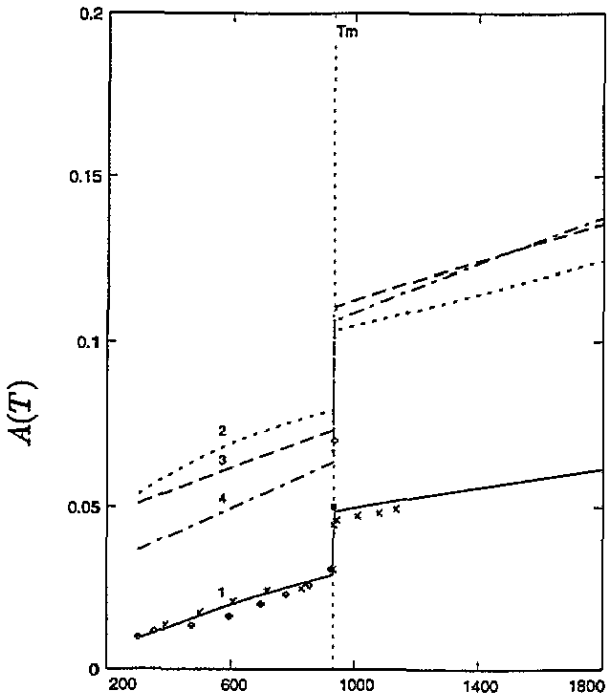

Figure 11. Total absorption in the solid and liquid state at $\lambda = 10.6\ \mu$m (1: ——), $\lambda = 1.064\ \mu$m (2: · · · · · ·), $\lambda = 0.53\ \mu$m (3: – – –) and $\lambda = 0.355\ \mu$m (4: — · —). The experimental values are taken from Brückner *et al* (1989) (◊) and from Schriempf (1974) (■) and Arnold (1984) (×).

increasing temperature is similar to the real part of the conductivity (figure 1). In the solid state, the main peak is essentially preserved and the increase at higher energies is mainly due to the Drude absorption. In the liquid state, the Drude absorption possesses a steep rise below 1 eV and is nearly exhausted at higher energies. A very broad contribution of the interband transitions appears above 1 eV. This is related to the non-vanishing optical mass and would, of course, vanish for $M = 1.0$, indicating a true free-electron-like behaviour.

The comparison with experimental reflection results (Shiles *et al* 1980 figure 2) shows a very good agreement up to $\omega \simeq 2$ eV. For higher energies, there is an almost constant difference of 3%. The reason is unclear, since neither an additional transition, as already discussed above, nor an additional ω-dependent scattering rate, as assumed by Dandrea and Ashcroft (1985), can lead to such a constant deviation.

The temperature dependence is represented for four relevant laser wavelengths, $\lambda_{CO_2} = 10.6\ \mu$m, $\lambda_{Nd} = 1.064\ \mu$m, $\lambda_{Nd}/2$ and $\lambda_{Nd}/3$, from room temperature up to $T = 1800$ K in figure 11. Unfortunately, we are not able to test the predictions of the theory in the solid state for wavelengths lying in the range of interband transitions. Taking into account the experimental uncertainty, the theoretical curve fits the CO_2 data (Arnold 1984, Brückner *et al* 1989, Schriempf 1974) very well. For the liquid state, Krishnan *et al* (1991) have measured absorption data with a nearly parallel growth the $\lambda_{Nd}/2$ curve but much lower

values. We have rejected their curve because the absorption values above the melting point are below the corresponding room-temperature result.

4. Conclusions

Though the proposed theory is simple enough to allow a calculation on simple personal computers, its results are in fairly good agreement with the experiments. This is, of course, to a large extent related to the simple electronic properties of the nearly-free-electron metal aluminium. But the separation of the conductivity into a Drude-like (intraband) and an interband part, which is dominated by the contributions of a few parallel one-electron bands, should be possible also for other polyvalent metals. From a purely theoretical point of view, the disadvantage of a semiphenomenological theory is the number of necessary experimental input parameters, However, we believe that this is balanced by its flexibility and the possibility of a fast computation of the frequency and temperature dependences of the optical properties.

It is worth while to note that not only is the theory capable of describing some selected optical properties but also it gives good agreement with all available experimental data.

The application of the theory to other polyvalent metals, indium and lead, for instance, is in preparation.

References

Alouani M and Khan M A 1986 *J. Physique* **47** 453
Arnold G S 1984 *Appl. Opt.* **23** 1434
Ashcroft N W 1963 *Phil. Mag.* **8** 2055
Ashcroft N W and Mermin N D 1976 *Solid State Physics* (Philadelphia: Saunders)
Ashcroft N W and Sturm K 1971 *Phys. Rev.* B **3** 1898
Benbow R L and Lynch D W 1975 1975 *Phys. Rev.* B **12** 5615
Bennett H E, Silver M and Ashley E J 1963 *J. Opt. Soc. Am.* **53** 1089
Brückner M, Schäfer J H and Uhlenbusch J 1989 *J. Appl. Phys.* **66** 1326
Brust D 1970 *Phys. Rev.* B **2** 818
Dandrea R G and Ashcroft N W 1985 *Phys. Rev.* B **32** 6936
Ehrenreich H 1966 *The Optical Properties of Solids* ed J Tauc (New York: Academic)
Ehrenreich H, Phillip H R and Segall B 1963 *Phys. Rev.* **132** 1918
Garik P and Ashcroft N W 1980 *Phys. Rev.* B **21** 391
Gathers G R 1983 *Int. J. Thermophys.* **4** 209
Gurzhi R N 1957 *Zh. Eksp. Teor. Fiz.* **33** 660 (1958 *Sov. Phys.–JETP* **6** 506)
Hafner J and Kahl G 1984 *J. Phys. F: Met. Phys.* **14** 2259
Holstein T 1952 *Phys. Rev.* **88** 1427
Iida T and Guthrie R I L 1988 *The Physical Properties of Liquid Metals* (Oxford: Oxford University Press)
Inagaki T, Arakawa E T, Caters A R and Glastad K A 1982 *Phys. Rev.* B **25** 6130
Jank W and Hafner J 1990 *Phys. Rev.* B **41** 1497
Klemperer O and Shepherd J P G 1963 *Adv. Phys.* **12** 355
Knight W D, Berger A G and Heine V 1959 *Ann. Phys., NY* **8** 173
Krishnan S and Nordine P C 1993a *Phys. Rev.* B **48** 4730
Krishnan S and Nordine P C 1993b *Phys. Rev.* B **47** 11 780
Krishnan S, Weber J K. Nordine P C, Schiffman R A, Hauge R H and Margrave J L 1991 *High Temp. Sci.* **30** 137
Mathewson A G and Myers H P 1972 *J. Phys. F: Met. Phys.* **2** 403
Miller J C 1969 *Phil. Mag.* **20** 1115
Oelhafen P, Indlekofer G and Güntherodt H J 1988 *Z. Phys. Chem. NF* **157** 483
Palik E D (ed) 1985, 1989 *Handbook of Optical Constants of Solids* (New York: Academic)
Powell C J 1968 *Phys. Rev.* **175** 972

Schriempf J T 1974 *NRL Report* 7728
Shiles E, Sasaki T, Inokuti M and Smith D Y 1980 *Phys. Rev.* B **22** 1612
Smith D Y and Segall B 1986 *Phys. Rev.* B **34** 5191
Smith D Y and Shiles E 1978 *Phys. Rev.* B **17** 4689
Smith D Y, Shiles E and Inokuti M 1985 *Handbook of Optical Constants of Solids* (New York: Academic)
Sturm K and Ashcroft N W 1974 *Phys. Rev.* B **10** 1343
Tups H and Syassen K 1984 *J. Phys. F: Met. Phys.* **14** 2753